Environ. Sci. Technol. **1999**, *33,* 1618−1626

Examination of the Size-Resolved and Transient Nature of Motor Vehicle Particle Emissions

M. MATTI MARICQ,*
DIANE H. PODSIADLIK, AND
RICHARD E. CHASE

Ford Motor Company, Research Laboratory, P.O. Box 2053, MD 3083, Dearborn, Michigan 48121

This paper reports mass measurements, size distributions, and the transient response of tailpipe particulate emissions from 21 recent model gasoline vehicles. Transient measurements are made for the FTP drive cycle (and limited ECE tests) using a scanning mobility particle sizer and an electrical low-pressure impactor. The particles emitted in vehicle exhaust have diameters in the 10−300 nm diameter range, with a mean diameter of about 60 nm. Particle emissions during the drive cycles occur as narrow peaks that correlate with vehicle acceleration. Cold start emissions generally outweigh those from a hot start by more than a factor of 3. Particulate mass deduced from the transient distributions agrees semiquantitatively with gravimetric measurements. Tailpipe particulate emissions from the recent model gasoline vehicles tested are very low, with mass emission rates ranging downward from 7 mg/mi for a light-duty truck during the cold start phase of the FTP drive cycle to ≤0.1 mg/mi during phase 2 for nearly half of the test vehicles. Three high-mileage (>100 K mi) test vehicles exhibited similarly low particulate emission rates. The FTP-weighted 3-bag average is under 2 mg/mi for all the conventional gasoline vehicles tested.

Introduction

Some recent epidemiological studies suggest a weak correlation between elevated ambient PM_{10} concentrations and increases in hospital admissions and death rates (*1*−*3*). Debate continues over the extent to which confounding pollutants affect the epidemiological link (*4*), and a causal relationship between particulate matter and cardiopulmonary health effects has not been identified. The correlation, however, has provoked sufficient environmental concern to lead to the new National Ambient Air Quality Standard for 2.5 μm particulate matter ($PM_{2.5}$) (*5*). The new standard represents an effort to address the issue that not all particles are alike and that they might not all have the same health effects. What the implications are for future emissions regulations is currently unknown, one of the difficulties being the lack of detailed information about the natures of the particles emitted from a number of important PM sources, motor vehicles included.

The available data suggest that motor vehicles contribute a significant, although not the major fraction, of PM_{10} (*6*−*9*). One estimate suggests that the combined motor vehicle emissions, roughly equally from tailpipe, brakes, tires, and secondary aerosol, constitutes 50−65% of the fine particle load in the Los Angeles area (*8*). Exhaust PM, which originates from incomplete combustion, and consists of soot coated by organic material and, in some cases sulfates, falls into the new $PM_{2.5}$ category. Earlier studies in this area concentrated primarily on diesel engines (*10*−*13*). Relatively little is known about particle formation by modern gasoline vehicles. Mass emission measurements have been made to develop a fleet emissions inventory for regulatory purposes (*14*), and only recently have efforts begun to address the question of particle size (*15*−*19*).

In an effort to broaden our understanding of vehicle particulate emissions, we have begun a program to investigate the size distributions of motor vehicle PM. The present paper describes our progress in this area. The techniques used for these measurements include the scanning mobility particle sizer (SMPS, used in a fixed size mode) and the electrical low-pressure impactor (ELPI). The purpose of this program is to investigate the numbers and sizes of tailpipe particles as well as the mass emissions. We extend the conventional "bag by bag" analysis to the examination of "second by second" variations in particle emissions rates. PM emissions are characterized with respect to size, number, and mass for 21 recent model, catalyst-equipped, gasoline vehicles as well as for a prototype ultralow emissions vehicle (ULEV) and a compressed natural gas (CNG) vehicle. Particle emissions from a direct injection spark ignition vehicle (DISI) and a diesel vehicle are presented for comparison, although these are current technology and do not represent emissions reduction technologies (e.g., particle traps) that are under development.

Experimental Method

Exhaust Dilution. The particulate emissions measurements were made at the Vehicle Emissions Research Laboratory (VERL) at Ford Motor Co. This facility is equipped with a 48-in. single roll, ac electric dynamometer, and a dual dilution tunnel whose flow is actively controlled to remain constant during a test. One tunnel is used for diesel vehicle tests; the other is reserved for low-emitting gasoline vehicles. Transient data on total hydrocarbon, CO, NO_x, and CO_2 gaseous emissions routinely accompany the particle measurements.

The dilution tunnels are constructed of 30.4 cm diameter electropolished stainless steel tubing. Dilution air is heated to 38 °C, filtered, and conditioned to low humidity (−9 °C dewpoint). Tunnel pressure is held to within 250 Pa of atmospheric pressure during the test. The flow rate of dilution air and the total flow of diluted exhaust are measured with subsonic venturis (smooth approach orifices). The tunnel operates in the turbulent flow regime, at a constant total flow set between 10 and 30 m^3/min, depending on the expected particulate emissions (10 m^3/min in the present study, except for the diesel vehicle). Two consequences of maintaining a constant total flow are that (i) the dilution ratio varies during the test cycle and (ii) the tailpipe particle emission rate is converted into tunnel particle concentration, the quantity measured by the SMPS and ELPI.

Exhaust is brought to the tunnel through a heated/insulated (T > 113 °C), corrugated, stainless steel tube with a diameter of 9.1 cm and a length of 5.8 m. Vehicle exhaust flow rates typically vary from about 0.1 m^3/min at idle to 2.5 m^3/min at the heavier accelerations during the FTP. The corresponding residence transfer line times vary from 20 to 1 s. The exhaust is introduced along the tunnel axis, near an orifice plate that ensures rapid mixing with the dilution air. Because the total flow is held constant (at 10 m^3/min), the

* Corresponding author phone: (313)594-7527; fax: (313)594-2923; e-mail: mmaricq@ford.com.

10.1021/es9808806 CCC: $18.00
Published on Web 04/01/1999

instantaneous dilution ratio, S_{air}/S_{exh}, varies from about 120 at idle to 2.5 at the heaviest accelerations (S_{air}/S_{exh} falls below 5 for about 25 s of the FTP drive cycle). Particle sampling occurs more than 10 tunnel diameters downstream to allow complete mixing of the exhaust and dilution air. At 10 m^3/s, the residence time of a particle in the tunnel is roughly 3 s. Secondary dilution, using an ejector pump diluter from Dekati (*20*), was employed for the diesel vehicle tests.

Particulate Matter Mass Measurement. Two drive cycles, driven by a robot driver, were used in this study: the U.S. UDDS (urban dynamometer drive schedule) (*21*) configured to constitute the three-phase FTP and a modified European cycle (*22*) ECE 15.05 (omitting the initial 40 s idle). Since they require a cold start, the tests were run over five consecutive days with data collected only on the last 4 days. For some vehicles, two such 5-day tests were performed. The post-test procedure consists of three coastdowns for the FTP (used to verify dynamometer performance) and three additional, 400-s, extra-urban phases for the ECE. The vehicles are soaked overnight in a temperature- and humidity-stabilized environment.

Particles for filter collection are sampled isokinetically at a rate of 0.66 L/s through a 1.1 cm diameter tube that makes a 20° bend with the tunnel flow axis. The 2-μm Teflo filters (47 mm diameter expanded PTFE Teflon) (*23*) are used to collect particles from each phase of the FTP test cycle (or the urban and extra-urban phases of the ECE cycle). The 2- and 1-μm filters additionally record the total emissions over the entire cycle. These are used to verify that collection efficiency does not depend on filter pore size and as a consistency check of the measurements for the individual phases of the drive cycles. Due to the high rated efficiency (>99%) of the Teflo filters, backup filters are not utilized. Particle emissions from four succeeding days of testing are integrated onto each filter. The filters are equilibrated with the room conditions for at least 2 h before both the pre- and post-collection weighing (on a Cahn C-33 microbalance). The filters weigh about 150 mg as compared to the 5−500 μg of particulate matter that is collected. A small correction, <1 μg, is made for tunnel background particulate matter originating from the filtered dilution air, which ranges from 0.3 to 0.8 $\mu g/m^3$. The errors in the final mass emission rates are about ±0.1 mg/mi.

Particle Size Instrumentation. Size- and time-resolved tailpipe particulate emission rates are measured using a model 3934 SMPS manufactured by TSI Inc. and the ELPI produced by Dekati Inc. (*20*). Vehicle exhaust is sampled using a 3/8-in. i.d. stainless steel tube inserted into the tunnel flow. The sampling is not strictly isokinetic, but this is not important for tailpipe particles, which lie almost entirely below 1 μm diameter. Large particles are removed at the entrance to the SMPS by a 577-nm 50% cutoff impactor. The remaining polydisperse aerosol is brought to a Boltzmann charge equilibrium by β-radiation from ^{85}Kr and passes through an electrostatic classifier. Here, particles experience an electrostatic force as well as an opposing viscous drag. These serve to separate particles according to their electrical mobility, which is a function of particle diameter. The size resolution of the instrument ranges from ±0.5 nm at 15 nm to ±30 nm at 500 nm at the classifier flow settings used in these experiments (0.4 L/min aerosol flow and 4.0 L/min sheath flow). Particles exiting the classifier are detected by a model 3010-S condensation nuclei counter (TSI, Inc.) having a response time of approximately 1 s.

The SMPS scan rate, a minimum of 30 s, is too slow to permit size distribution measurements during the FTP, where transients occur on a <1 s time scale. Instead, the voltage on the classifier is fixed to transmit a narrow distribution of particle sizes throughout the drive cycle. Four to eight such time traces at fixed sizes in the 20−500 nm diameter range are combined to construct three-dimensional particle number versus size versus time distributions. For each trace, the raw particle count rate, $C(t,D_p)$, is recorded at 2-s intervals and converted to a differential tailpipe emission rate via

$$\frac{dN(t)}{d\ln(D_p)} = \frac{C(t,D_p)T(D_p)q_T}{q_a f(+1)\epsilon_i\epsilon_c}e^{\alpha C} \quad (1)$$

where $N(t)$ represents the tailpipe particles per second, $T(D_p)$ is the transmission function of the classifier (approximated as a triangle, $2/\Delta(\ln D_p)$), q_T is the tunnel flow, q_a is the aerosol sample flow, $f(+1)$ is the size-dependent fraction of +1 charged particles, and ϵ_c and ϵ_i are the efficiencies of the condensation nuclei counter and the impactor at the classifier entrance. The factor $e^{\alpha C}$ represents a coincidence correction for high particle count rates ($\alpha = 4 \times 10^{-7}$ s).

The ELPI separates particles according to aerodynamic size using a Berner low-pressure cascade impactor operating at approximately 100 mTorr and a flow rate of 10 L/min (*24*). Twelve stages cover the size range of 48 nm−8.6 μm (midpoint diameters). Transient operation, with a time resolution of 1 s, is achieved by first charging the aerosol in a corona discharge and then recording the current deposited on each impactor stage. The electrical currents are converted into particle number (or volume) rates using the known dependence of charging efficiency on particle size and correcting for diffusional and electrostatic losses of small particles as they pass through the cascade impactor. As seen below, good agreement with SMPS measurements is observed, except for the lowest ELPI stage (the results from which are not used).

Measurements of the test cell air (the source of vehicle intake and dilution air) reveal an accumulation mode peak (sometimes a bimodal distribution is observed) with a maximum in the 100−200 nm range. The number concentration is typically about 3×10^9 m^{-3}, which corresponds to 15 $\mu g/m^3$ in the fine particle mode (<0.6 μm) assuming $\rho =$ 1 g/cm^3. After filtering, the number concentration, broadly peaked at ~100 nm, drops to roughly 4×10^8 m^{-3}, and the corresponding mass concentration falls to nearly 1 $\mu g/m^3$. The consistency of the latter value with the 0.3−0.8 $\mu g/m^3$ measured by filter collection indicates that coarse mode particles are effectively removed from the dilution air.

Results

Transient Size Distributions: Repeatability. Table 1 describes the vehicles included in this study. Most of the vehicles were low mileage (<10 K mi); however, three had over 100 K mi. The U.S. cars were run on either EPA certification fuel or California Phase II reformulated fuel, whereas the European automobiles were tested with European reference fuel, RF08A. Table 2 lists the gaseous total hydrocarbon, CO, NO_x, and CO_2 emissions for each vehicle as a weighted average over the relevant drive cycle. The table serves two purposes: (i) the data characterize the operation of the engine and exhaust aftertreatment and (ii) they provide a useful context within which to examine the particulate emissions.

The inability of the SMPS to scan on the time scale of the FTP transients and the requirement of a cold start limit the particle emissions measurements to one narrow size region within the full 10−500 nm range per day. This means that an entire three-dimensional map of particle emission rate as a function of size and time along the drive cycle requires 4−8 days, or more, of vehicle tests. It naturally brings up the question of how repeatable the particle emission rates from a particular vehicle are from day to day. As Figure 1 demonstrates, the reproducibility of PM emissions is actually very good. The lower set of traces shows the raw particle data obtained with the SMPS for three measurements on separate days of 75 ± 4 nm particles from vehicle T1 during

TABLE 1. Description of Vehicles and Tests

vehicle[a]	year	cyl[b]	test fuel	odometer miles	transmission	test type
T1	1997	6	EPA cert.	<8 000	automatic	FTP
T2	1996	6	EPA cert.	<8 000	automatic	FTP
T3	1995	6	EPA cert.	2 600	automatic	FTP
T4	1997	6	EPA cert.	35 500	automatic	FTP
T5	1997	6	CA ph 2 refrm	4 200	automatic	FTP
T6	1995	6	CA ph 2 refrm	150 500	automatic	FTP
T7a	1996	6	CA ph 2 refrm	5 461	automatic	FTP
T7b	1996	6	CA ph 2 refrm	2 900	automatic	FTP
T8	1995	6	CA ph 2 refrm	9 500	automatic	FTP
C1a	1996	6	CA ph 2 refrm	5 346	automatic	FTP
C1b	1996	6	CA ph 2 refrm	100 200	automatic	FTP
C2	1997	6	CA ph 2 refrm	3 500	automatic	FTP
C3	1996	4	CA ph 2 refrm	5 656	automatic	FTP
C4	1997	4	CA ph 2 refrm	4 200	automatic	FTP
C5	1996	8	CA ph 2 refrm	<6 000	automatic	FTP
C6	1997	8	EPA cert.	10 100	automatic	FTP
C7	1998	8	CA ph 2 refrm	104 000	automatic	FTP
EC1	1994	4	RF08A		5 spd manual	FTP & ECE
EC2	1995	4	RF08A		5 spd manual	modified ECE
EC3a	1995	6	RF08A		automatic	modified ECE
EC3b	1995	6	RF08A		automatic	modified ECE
prototype ULEV	1994	8	EPA cert.	10 600	automatic	FTP
CNG	1996	8	CNG		automatic	FTP
DISI	1997	4	EPA cert.	7 060	automatic	FTP
diesel	1995	4		12 200	5 spd manual	FTP

[a] T, light-duty gasoline truck; C, gasoline automobile; EC, European gasoline automobile; ULEV, ultralow emitting vehicle; CNG, compressed natural gas; DISI, direct injection gasoline. [b] Number of cylinders.

TABLE 2. Average Regulated Gaseous Emissions

vehicle[a]	test	THC (g/mi)	CO (g/mi)	NO_x (g/mi)	CO_2 (g/mi)	NMHC (g/mi)
tier I std[b] truck >3750 lb			4.4	0.700		0.320
T1	FTP	0.115	1.00	0.043	486	0.102
T2	FTP	0.107	0.87	0.126	453	0.092
T3	FTP	0.089	1.14	0.043	468	0.079
T4	FTP	0.081	1.35	0.049	451	
T5	FTP	0.091	0.90	0.094	422	0.083
T6[c]	FTP	0.174	3.45	0.688	414	0.139
T7a	FTP	0.092	1.06	0.077	507	0.081
T7b	FTP	0.151	1.12	0.165	543	0.140
T8	FTP	0.163	1.95	0.072	451	0.148
tier I std[b] cars		0.410	3.4	0.400		0.250
C1a	FTP	0.139	1.16	0.140	405	0.123
C1b[c]	FTP	0.172	1.79	0.530	385	0.153
C2	FTP	0.183	0.96	0.045	457	0.165
C3	FTP	0.073	1.08	0.080	314	0.066
C4	FTP	0.062	0.64	0.040	307	0.057
C5	FTP	0.085	0.91	0.060	465	0.077
C6	FTP	0.113	0.36	0.264	458	0.103
C7[c]	FTP	0.180	1.37	0.198	457	0.157
prototype ULEV	FTP	0.053	0.65	0.129	524	0.045
CNG	FTP	0.074	0.51	0.021	402	0.011
EC1	FTP	0.230	2.58	0.057	316	na
EC1	ECE	0.396	2.04	0.143	326	na
EC2	ECE	0.456	2.32	0.138	317	na
EC3a	ECE	0.604	2.29	0.360	469	na
EC3b	ECE	0.474	2.38	0.688	488	na
DISI	FTP	0.326	3.64	0.162	294	na
diesel	FTP	na	0.49	0.741	306	na

[a] T, light-duty gasoline truck; C, gasoline automobile; EC, European gasoline automobile; ULEV, ultralow emitting vehicle; CNG, compressed natural gas; DISI, direct injection gasoline; na, not available. [b] All U.S. vehicles met, at a minimum, the listed tier I regulated levels. Some met more stringent standards. [c] High mileage vehicle, >100 000 miles.

the cold start (phase 1) portion of the FTP cycle. Displaced for clarity (and scaled by a factor of 10) are two traces of 85 ± 5 nm particle emissions from vehicle C5 during phase 1. Both sets of measurements reveal marked variations of particle formation rates over the course of the drive cycle; yet, in each case the times and levels of the emissions are accurately duplicated from one day to the next. The deviations in the 10 most prominent peaks range from 0 to 50%; on average they agree within 16%.

Figure 2 compares, for vehicle T5, three transient size distributions recorded using the ELPI and a SMPS-based distribution constructed from 7 days of tests. The top two panels show ELPI data over the 30−350 nm size range; panel 3 displays data over a reduced range of 65−350 nm. All three data sets indicate reproducibility equivalent to the SMPS traces in Figure 1; namely, individual peak heights agree within 50%, and the average deviation lies within 15%. The comparison between the first two ELPI data sets and the third one indicates that the number-weighted distributions are dominated by the 34−65 nm particles collected on the lowest impactor stage. Below, in Figure 6, good agreement is demonstrated between time-integrated ELPI and SMPS size distributions, except for the lowest ELPI stage. Overestimation by this stage, which occurs near the maximum of the size distribution, is one reason the peak amplitudes in panels 1 and 2 appear so much bigger than their SMPS counterparts. Removal of the lowest stage ELPI data in panel 3 significantly improves the agreement. The peaks remain more intense, because the peak widths in the ELPI data are about two-thirds of the widths in the SMPS data owing to the faster time response of the ELPI.

A detailed comparison between ELPI and SMPS particle size distributions is beyond the scope of this paper (*25*). One complication is that the ELPI measures the particle's aerodynamic size, whereas the SMPS gives its mobility size; thus, a strict comparison requires accounting for the particle's density (*26*). Assuming that the particulate emissions are primarily carbonaceous, their density should not differ very much from 1 g/cm^3. To a reasonable approximation, therefore, the mobility and aerodynamic diameters are comparable, which is consistent with the similarity between the ELPI and SMPS distributions in Figure 2.

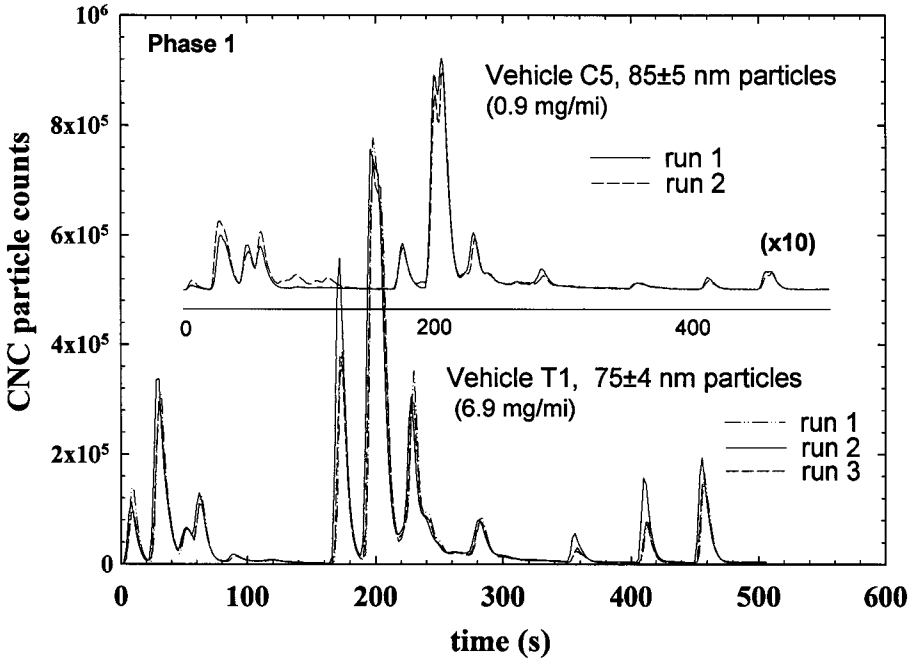

FIGURE 1. Test-to-test variability of transient, size-selected, tailpipe particulate emissions during the cold start, phase 1, of the FTP drive cycle. The measurements are made using the SMPS. Vehicle C5 traces are displaced vertically and horizontally from vehicle T1 data for clarity.

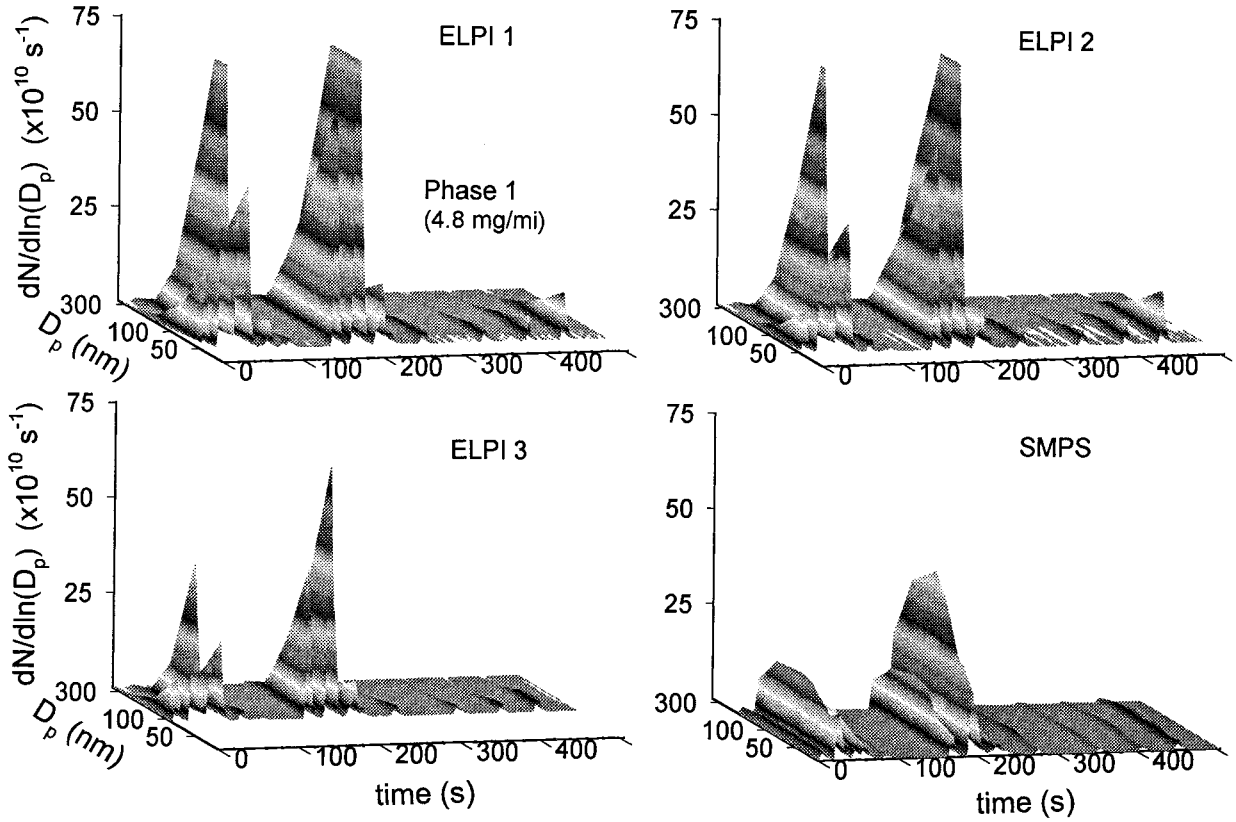

FIGURE 2. Reproducibility of transient particle size distributions for vehicle T5 driven over phase 1 of the FTP. A composite distribution from SMPS data is compared to three ELPI distributions. Note that the ELPI data extends down to 48 nm (midpoint of 34−65 nm stage) in panels 1 and 2 and only to 87 nm in panel 3, whereas the SMPS data is plotted to 29 nm.

Characteristics of Particle Emissions: Time and Size. It is evident from Figures 1 and 2 that tailpipe particle emission rates from spark ignition vehicles are small except at several succinct times during the drive cycle. This is further illustrated by Figure 3, which compares cold start versus hot start PM emissions during phases 1 and 3 of the FTP. There are a number of noteworthy points regarding these data. First, the particle emissions occur during vehicle acceleration, as is apparent from comparing the peaks in particulate emissions to the vehicle speed traces shown along the rear faces of the plots in Figure 3. This correlation is ubiquitous to the gasoline vehicle tests reported herein. The peaks are prominent during phases 1 and 3 of the FTP and during the urban portion of the ECE cycle, but in many cases they disappear into the

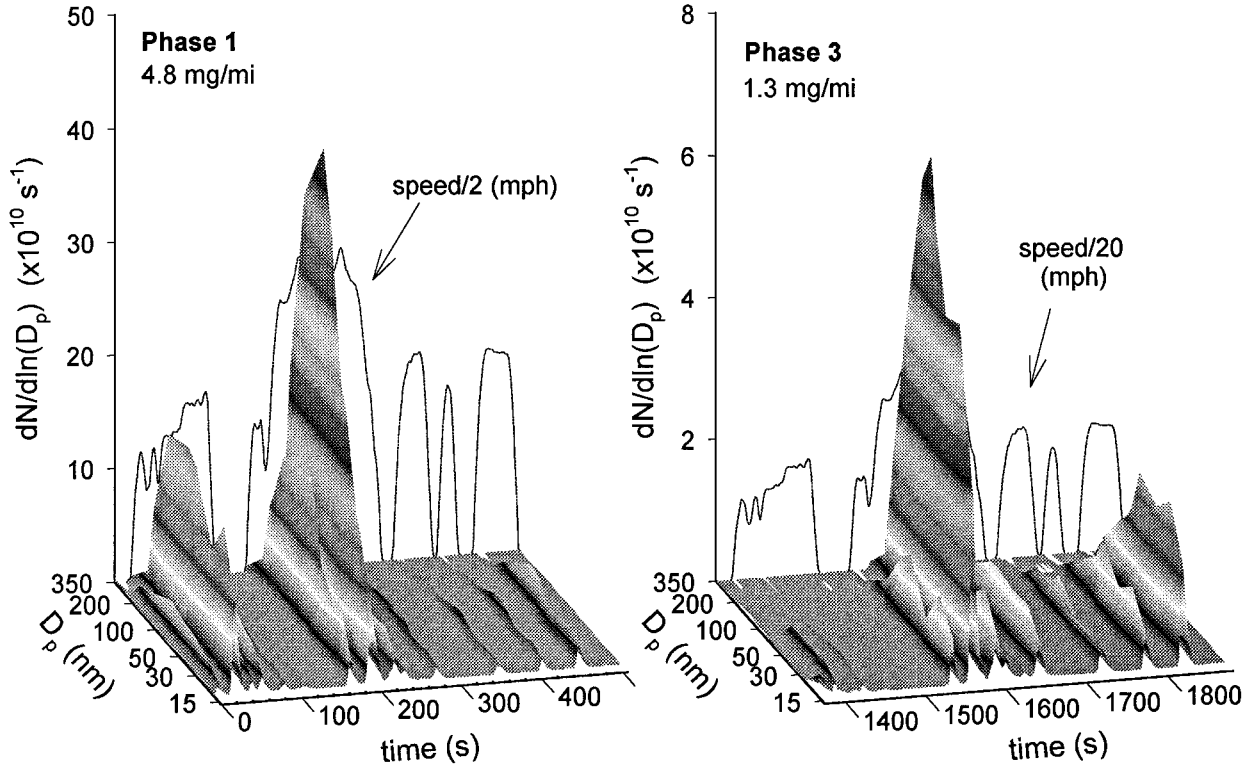

FIGURE 3. Comparison of size-resolved particle emissions from a gasoline light-duty truck (T5) during the cold start (phase 1) versus the hot start (phase 3) of the FTP. Note the change in vertical scale from phase 1 to phase 3. Vehicle speed is shown by the traces along the rear walls of the plots.

noise during phase 2 of the FTP and the extra-urban phase of the ECE.

In the absence of vehicle exhaust, the tunnel background particle concentration of 4×10^8 m^{-3} is about 10 times lower than ambient. This corresponds to a differential particle rate of d N/d ln $D_p \sim 2 \times 10^7$ s^{-1} at a diameter of 75 nm and a tunnel flow of 10 m^3/min. Relative to this background, the peak particle emission rates during heavy accelerations can climb by over 3 orders of magnitude, whereas during the majority of the drive cycle, between emission episodes, the particulate emission rates vary only from 1 to 10 times the tunnel background level. In contrast, the emission peaks for the DISI and diesel vehicles are noticeably broader in time, and the particle levels in the troughs between peaks remain over 2 orders of magnitude above tunnel background.

A second point illustrated by Figures 2 and 3 is that the emission rates are dominated, in terms of particle number, by fine and ultrafine particles with diameters in the range of 10−300 nm. The details in the shapes of the distributions as well as the overall emission rates (see Table 3) vary with vehicle model. It is also true that a given vehicle can exhibit substantially different particle emission rates when driven over different test cycles. Thus, in Table 3, the number of particles emitted during phase 3 of the FTP range from being comparable to those for phase 2 to exceeding them by a factor of 40. The corresponding mass emissions exhibit a similar but more subdued dependence on drive cycle. It is reasonable to surmise that the higher emissions recorded for phase 3 versus phase 2 of the FTP occur because of the higher speeds and accelerations that take place; however, the precise reasons why acceleration leads to particle formation deserve a more careful examination.

There are three, perhaps more, ways of looking at particulate emissions. We have chosen to report number- and mass-weighted emission rates, either as particles per second exiting the tailpipe or as milligrams per mile. These are the "bottom line" quantities relevant to emissions inventories and source apportionment. They are also the quantities directly measured when sampling particles from a tunnel flow that is held constant. To the engineer interested in improving engine performance, however, exhaust gas particle concentration (number- or mass-weighted) or particles per unit fuel consumed might be the more informative quantities. In fact, the peaks in particle emission rates, evident in Figures 1−3, have at least two possible origins: one is the increase in exhaust flow that occurs during acceleration and the second is an increase in the concentration of particles formed during combustion (others might include reduced catalyst efficiency, etc.). The first factor is relevant because the dilution tunnel operates in a constant total flow mode; thus, the dilution ratio decreases with increasing exhaust flow. Since the exhaust flow varies only by a factor of 5−20 over the FTP, the 10^3-fold increases in particulate emissions observed during the more strenuous accelerations cannot be attributed solely to the larger flow of air and fuel through the engine. Rather the extent of particle production per unit amount of fuel burned substantially increases during these times.

This idea is substantiated by Figure 4. The differential particle concentration in the exhaust of vehicle T5 is determined from the differential rate (i.e., the tunnel particle concentration) by dividing the latter quantity by the exhaust flow, measured as the difference in total tunnel flow and dilution air flow. It is apparent that increases in particle formation during vehicle acceleration, and not just increases in exhaust flow, are responsible for the peaks in particulate emissions observed along the transient drive cycles (note that the spikes marked with asterisks are artifacts from unrealistically low exhaust flow measurements at some points).

A comparison of the two plots in Figure 3 and the particle number emissions listed in Table 3 reveals that particulate emissions during phase 1 are typically an order of magnitude higher than those for phase 3 of the FTP, even though the

TABLE 3. Particulate Matter Emissions

vehicle[a]	phase	N ($\times 10^{12}$)	mean diameter[b] (nm)	σ [c]	M_T (mg/mi)	filter mass[e] (mg/mi)
T1	1	51 ± 13	70 ± 14	0.6 ± 0.2	14 ± 15	6.9
	2	0.6 ± 0.4	48 ± 32	0.8 ± 0.7	0.2 ± 0.9	0.1
	3	13 ± 2	45 ± 3	0.7 ± 0.1	1.8 ± 1.0	1.5
T2	1	34 ± 5	81 ± 9	0.6 ± 0.1	15 ± 9	4.6
	2	0.3 ± 0.1	82 ± 18	0.6 ± 0.2	0.2 ± 0.2	0.2
	3	1.8 ± 0.5	64 ± 11	0.5 ± 0.2	2 ± 2	0.6
T3	1	5.9 ± 0.6	63 ± 5	0.6 ± 0.1	1.0 ± 0.5	0.9
	2	2.0 ± 0.1	57 ± 7	0.4 ± 0.1	0.08 ± 0.03	0.3
	3	1.7 ± 0.4	69 ± 8	0.4 ± 0.1	0.12 ± 0.09	0.4
T4	1	23 ± 7	65 ± 8	0.6 ± 0.1	4 ± 3	0.7
	2	0.6 ± 0.2	61 ± 11	0.7 ± 0.2	0.1 ± 0.1	0.1
	3	0.9 ± 0.2	45 ± 9	0.7 ± 0.2	0.1 ± 0.1	0.2
T5	1	24 ± 4	71 ± 9	0.7 ± 0.1	10 ± 9	4.8
	2	0.5 ± 0.2	45 ± 17	0.9 ± 0.4	0.3 ± 0.5	0.4
	3	3.1 ± 0.3	47 ± 5	0.8 ± 0.1	0.8 ± 0.5	1.3
T6	1	8 ± 2	57 ± 4	0.5 ± 0.1	0.5 ± 0.3	1.6
	2	0.5 ± 0.3	50 ± 23	0.7 ± 0.4	0.1 ± 0.2	0.0
	3	1.6 ± 0.7	57 ± 16	0.6 ± 0.3	0.3 ± 0.4	1.1
T7a	1	2.7 ± 0.7	49 ± 8	0.6 ± 0.2	0.3 ± 0.4	0.9
	2	0.2 ± 0.2	61 ± 32	0.7 ± 0.7	0.04 ± 0.15	0.1
	3	0.4 ± 0.1	84 ± 15	0.4 ± 0.3	0.06 ± 0.04	0.3
T7b	1	14 ± 2	63 ± 6	0.7 ± 0.1	5 ± 3	1.6
	2	0.07 ± 0.03	51 ± 20	0.9 ± 0.4	0.2 ± 0.5	0.1
	3	0.07 ± 0.02	37 ± 15	1.0 ± 0.4	0.1 ± 0.1	0.2
T8	1	26 ± 5	62 ±7	0.5 ± 0.1	4 ± 2	
	2	0.4 ± 0.1	42 ± 12	0.7 ± 0.3	0.05 ± 0.09	
	3	0.6 ± 0.3	53 ± 21	0.7 ± 0.5	0.2 ± 0.4	
C1a	1	13 ± 1	64 ± 32	0.8 ± 0.7	1.7[d]	1.8
	2					0.4
	3	1.0 ± 0.2	136 ± 15	0.6 ± 0.2	3 ± 2	0.6
C1b	1	17 ± 2	66 ± 6	0.6 ± 0.1	4 ± 3	2.3
	2					0.0
	3	3 ± 1	76 ± 7	0.5 ± 0.1	0.4 ± 0.2	0.4
C2	1	18 ± 2	67 ± 4	0.6 ± 0.1	2 ± 1	2.5
	2	0.12 ± 0.06	80 ± 13	0.5 ± 0.2	<0.1	0.1
	3	0.12 ± 0.06	57 ± 18	0.6 ± 0.3	<0.1	0.3
C3	1	4.1 ± 1.0	66 ± 10	0.6 ± 0.2	0.4 ± 0.4	0.4
	2	0.3[d]			0.08[d]	0.1
	3	0.7[d]			0.34[d]	0.3
C4	1	12 ± 3	70 ± 6	0.6 ± 0.1	2.7 ± 1.3	<0.7
	2	0.3 ± 0.1	65 ± 7	0.4 ± 0.1	0.03 ± 0.02	
	3	0.7 ± 0.2	70 ± 6	0.3 ± 0.1	0.05 ± 0.03	
C5	1	2.6 ± 0.3	64 ± 5	0.5 ± 0.1	0.3 ± 0.1	0.9
	2	0.07 ± 0.02	60 ± 8	0.7 ± 0.1	0.02 ± 0.01	0.7
	3	3.1 ± 01.4	107 ± 10	0.3 ± 0.2	0.7 ± 0.3	0.5
C6	1	42 ± 4	67 ± 4	0.6 ± 0.1	7 ± 3	5.2
	2	0.2 ± 0.05	87 ± 31	0.6 ± 0.4	0.2 ± 0.3	0.3
	3	0.9 ± 0.4	63 ± 20	0.8 ± 0.4	0.6 ± 1.6	0.2
C7	1	6.6 ± 1.0	50 ± 10	0.8 ± 0.2	0.8 ± 0.9	1.1
	2	0.02[d]			<0.1[d]	0.1
	3	0.05 ± 0.02	50 ± 10	1.1 ± 0.6	<0.1[d]	0.3
EC1	1	15[d]			3[d]	2.1
	2	1.1[d]			0.3[d]	0.2
	3					0.7
	urban	3.6 ± 0.2	71 ± 3	0.4 ± 0.1	0.7 ± 0.2	0.8
	extra	1.8 ± 0.1	71 ± 4	0.4 ± 0.1	0.2 ± 0.05	1.3
EC2	urban					1.1
	extra					1.7
EC3a	urban	13 ± 5	91 ± 19	0.5 ± 0.2	6 ± 6	2.9
	extra	1.1 ± 0.7	66 ± 23	0.5 ± 0.3	0.1 ± 0.2	1.1
EC3b	urban	13 ± 3	81 ± 10	0.6 ± 0.2	7 ± 5	2.9
	extra	0.3 ± 0.04	86 ± 5	0.5 ± 0.1	0.07 ± 0.03	1.2
prototype	1	3.9[d]			0.3[d]	0.6
ULEV	2	0.2 ± 0.1	68 ± 15	0.5 ± 0.3	0.01 ± 0.02	0.1
	3	0.8 ± 0.2	101 ± 18	0.7 ± 0.2	0.8 ± 0.6	0.5
CNG	1	0.4[d]			0.05[d]	1.1
	2	0.2[d]			0.04[d]	0.3
	3	0.5[d]			0.11[d]	0.6
DISI	1	87 ± 20	90 ± 13	0.6 ± 0.1	42 ± 33	22
	2	100 ± 33	85 ± 18	0.6 ± 0.2	39 ± 45	20
	3	60 ± 20	77 ± 15	0.6 ± 0.2	21 ± 26	11

TABLE 3 (Continued)

vehicle[a]	phase	N ($\times 10^{12}$)	mean diameter[b] (nm)	σ [c]	M_T (mg/mi)	filter mass[e] (mg/mi)
diesel	1	550 ± 62	76 ± 5	0.6 ± 0.1	160 ± 70	113
	2	670 ± 86	70 ± 6	0.5 ± 0.1	110 ± 50	71
	3	470 ± 92	76 ± 9	0.6 ± 0.1	140 ± 120	91

[a] Vehicles labeled as in Tables 1 and 2. [b] Mean of log-normal particle size distribution (eq 1), equivalently geometric mean size, with 95% confidence limits. [c] Standard deviation (width) of log-normal size distribution with 95% confidence limits. [d] Total number and mass obtained by numerical integration of measured size distribution, not by fitting to a log-normal distribution. [e] Mass measurement uncertainty is ±0.1 mg/mi.

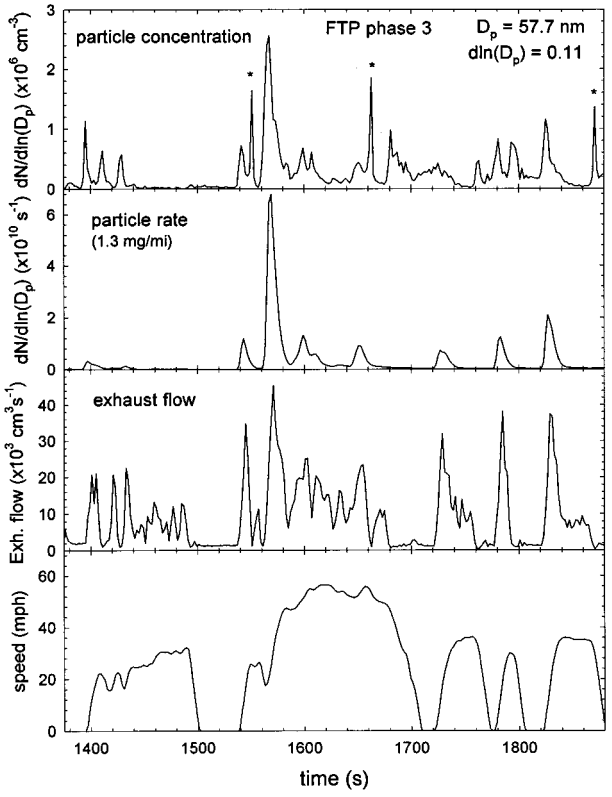

FIGURE 4. Two views of tailpipe particle emissions during phase 3 of the FTP. The top panel shows particle concentration in the exhaust gases of vehicle T5. The second panel gives the particle rate exiting the tailpipe. The exhaust flow rate and vehicle speed are depicted in panels 3 and 4, respectively. The asterisks in the top panel mark possible artifacts originating from momentarily very low apparent exhaust flows.

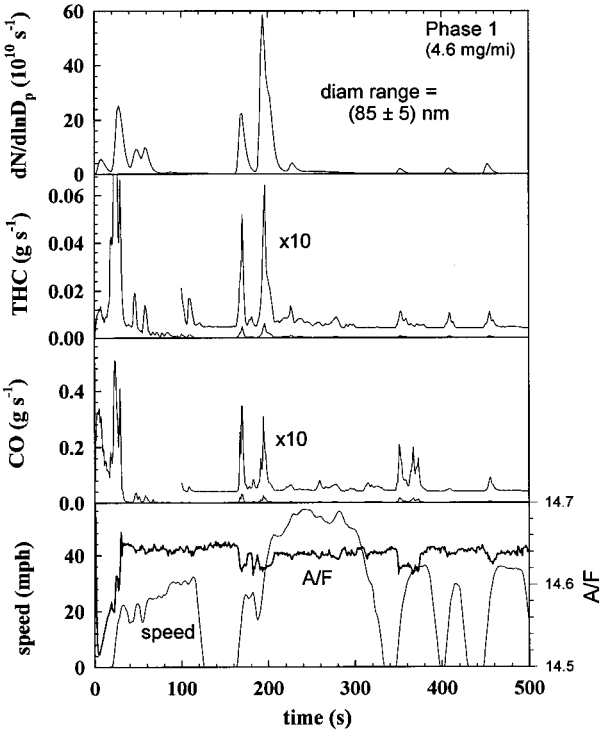

FIGURE 5. Comparison of particulate, gaseous hydrocarbon, and carbon monoxide emissions from vehicle T2 over phase 1 of the FTP. Also shown in the bottom panel are the vehicle speed and air-to-fuel ratio.

speed traces are identical. The particulate mass data, also provided in Table 3, corroborate the higher emissions during the cold start, with phase 1:phase 3 mass ratios ranging from 1.2 to 7.4. The difference between these two phases of the FTP is that the first has a cold start whereas the other follows a hot start. This leads to the conclusion that warming of the engine and/or catalyst to operating temperature has a significant effect on the rate of particles emitted from the tailpipe (*27*).

The pattern of particulate emissions during the drive cycle mirrors the behavior observed for total hydrocarbon and CO emissions. This is perhaps not surprising since in each case the emissions result from incomplete combustion. Figure 5 compares particulate to gaseous emissions. For each species, emission rates are peaked and coincident with acceleration of the vehicle. Furthermore, they correlate with excursions of the air/fuel ratio toward richer mixtures. It is apparent, however, that hydrocarbon and CO emissions exhibit a more dramatic decrease after catalyst lightoff, which occurs about 50 s into the phase 1 portion of the test, than do particle emissions. This suggests that the catalyst efficiency for particulate removal is lower than it is for gas-phase hydrocarbons.

Number-Based versus Filter-Based Particulate Mass. The SMPS and ELPI provide real time data on the number densities of particles emitted by the test vehicle. While these provide insight into the issue of particulate emissions, regulations are written in terms of particle mass, and measurements are historically mass based. It is, thus, of interest to extract the equivalent total mass emissions from the transient particle number and size data. This is accomplished by integrating time-dependent distributions, such as illustrated in Figures 2 and 3, over each phase of the driving cycle. These summed distributions, owing to the limited number of sizes at which data are collected, are assumed to fit a log-normal form

$$f(\ln(D_p)) = \frac{N}{\sigma 2^{1/2}\pi^{1/2}} \exp[-(\ln(D_p) - \ln(\mu))^2/(2\sigma^2)] \quad (2)$$

as shown in Figure 6. Here, $\ln(\mu)$ and σ are the mean and standard deviation of the distribution and N represents the total number of particles emitted from the tailpipe during the test phase under consideration (μ is the geometric mean size). Where available, SMPS and ELPI data are combined

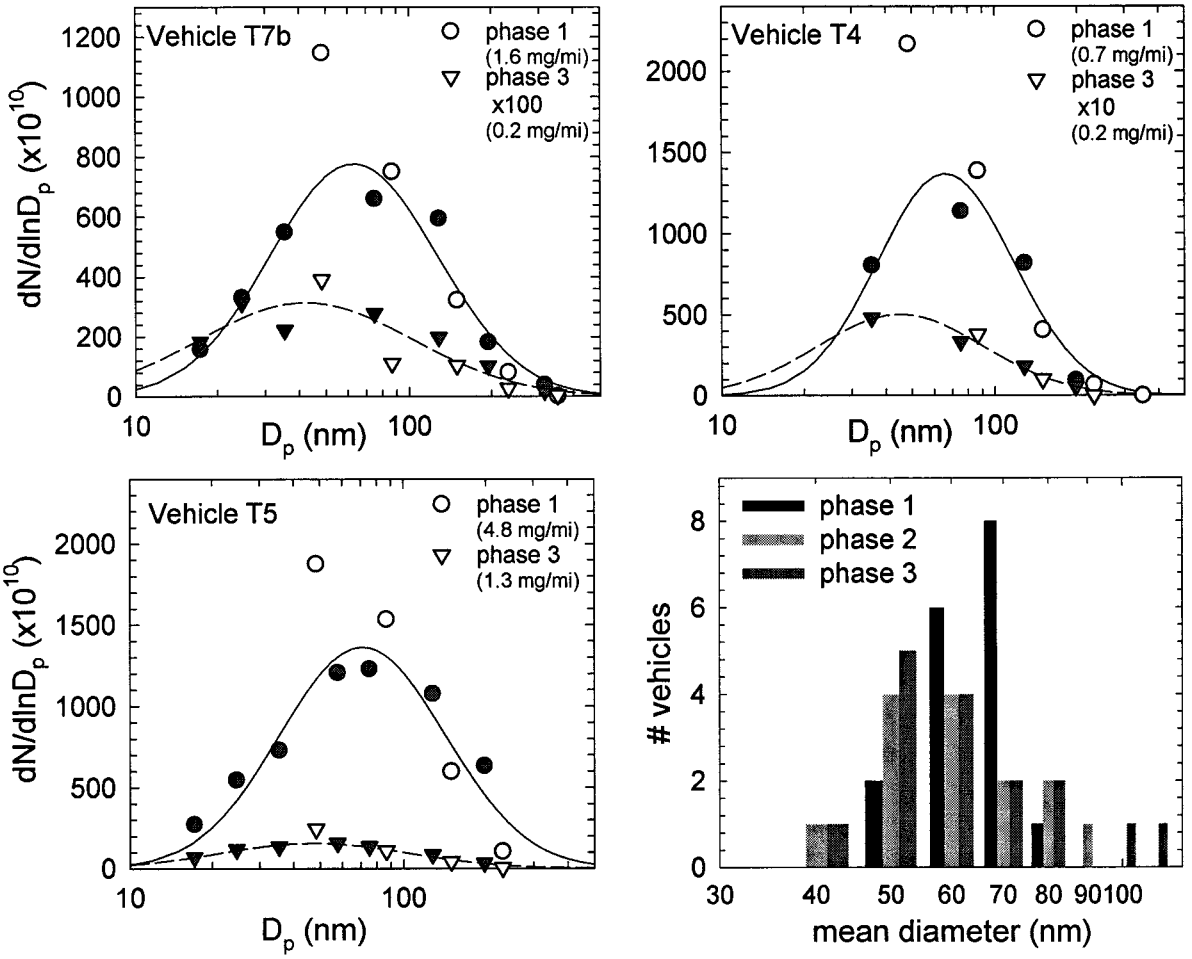

FIGURE 6. (Panels 1−3) Examples of time-integrated particle size distributions for phases 1 and 3 of the FTP. Open symbols denote ELPI data, and filled symbols represent SMPS data. The smooth lines represent fits to the log-normal distribution (omitting the lowest ELPI stage data). (Panel 4) Distributions for phases 1−3 of the FTP of mean particle size for all gasoline vehicles tested.

for the fits, except that data from the smallest (48 nm) stage of the ELPI, which appears systematically to overestimate the particle number, are omitted. The resulting particle number emissions and mean sizes for each test vehicle are listed in Table 3.

Mass-weighted distributions can be derived from their number-weighted counterparts in two ways: The straightforward method is to assume the particles to be spherical and then weight each point in the distribution by the corresponding volume and density. The drawback to this procedure is that it requires accurate knowledge of the particle emissions at the large diameter tail of the distribution. In the current circumstances, this is hindered both by the lack of data points in this size range and by the statistical noise present in the data that are available (from the low count rates of large particles). An alternative is to utilize the log-normal distribution as an interpolating function. It gives a physically reasonable description of the number of particles as a function of diameter in an aerosol sample. Though exhaust PM emissions can differ significantly from log-normal, the examples in Figure 6 show that they are often reasonably well approximated by this distribution.

Mass weighting the log-normal approximation and integrating this distribution over particle size yields

$$M_T = \frac{N\rho\pi}{6}\mu^3 \exp(9\sigma^2/2) \qquad (3)$$

where ρ is the particle density. Estimates of PM mass emissions derived from SMPS and ELPI data via eq 3 are compared to the results of filter measurements in Table 3. The agreement is semiquantitative due to the 50−100% error bars in M_T. These are large because small uncertainties in the tail of the size distribution, due to the fitting errors in N, μ, and σ, have a disproportionally large influence on PM mass.

On an absolute basis, the errors in M_T are too big to permit a quantitative comparison with the gravimetric measurements. However, on a relative basis they serve a useful purpose. Both size distribution and filter-derived data are consistent in that recent model gasoline vehicle PM emission rates are small, $<\sim$10 mg/mi, as compared to (a) the current regulation of 80 mg/mi, (b) diesel PM emissions of $\sim$90 mg/mi, and (c) DISI emissions of $\sim$18 mg/mi. Both methods are also consistent in indicating higher emissions during phase 1 (cold start) as compared to phases 2 and 3 of the FTP. Because the SMPS instrument does not explicitly count particles with diameters larger than $\sim$0.6 μm, the consistency between SMPS-derived and filter-based mass emissions indicates that the particulate matter collected on the filters is, in fact, in the 10−300 nm diameter range, and that the mass does not arise from a small population of "large" particles with diameters near 1 μm or larger.

Discussion

The present study establishes that it is feasible to make reliable and reproducible transient measurements of particle size distributions for gasoline vehicles. The majority of particles range from about 10 to 300 nm in diameter, based on a number-weighted distribution. The (geometric) mean di-

ameters for the gasoline test vehicles range from 45 to 80 nm, with a few outliers, as shown in the fourth panel of Figure 6. The mean diameter is larger for the cold start phase, about 65 nm, as compared to phases 2 and 3 of the FTP, roughly 55 nm. This could be due to higher amounts of condensed semivolatile organic material or reduced fragmentation due to the lower engine temperature. The corresponding mass-weighted mean diameters are in the vicinity of 200 nm, placing engine exhaust particles well within the new $PM_{2.5}$ category.

Because particles are affected by coagulation, condensation, and nucleation processes, the question arises of whether the dilution tunnel measurements are representative of the actual exhaust particulate emissions (*28*). A recent comparison between direct tailpipe sampling and dilution tunnel measurements of gasoline vehicle PM shows them to be the same (though PM artifacts can arise from very hot exhaust at high speed and load) (*29*). The relatively low particle number in gasoline vehicle exhaust makes coagulation en route to the tunnel inefficient, and removal of gaseous hydrocarbons by the catalyst reduces condensation and nucleation rates. These particle processes can play a role, however, in dilution tunnel studies of diesel emissions.

The transient particle measurements reveal that spark ignition vehicles emit particles principally during very specific short-time durations during the driving cycle. These times coincide with periods of relatively heavy acceleration, during which peaks in hydrocarbon and CO emissions are likewise observed. The level of particulate emissions does not correlate with engine displacement or vehicle mileage. Some light-duty trucks have particulate levels comparable with those of the lower emitting automobiles, both on a mass and number basis. And the limited number of high-mileage vehicles tested have PM emissions comparable to the average low-mileage vehicle. These observations suggest that control of parameters such as fuel injection, spark timing, and air-to-fuel ratio during acceleration may be important in determining the extent of particulate formation.

The tailpipe particulate mass emissions measured from the recent model gasoline test vehicles are very low, including the three high-mileage vehicles. For phase 1 (cold start), they extend from 0.4 mg/mi for a 1996 car to 6.9 mg/mi for a 1997 light-duty truck. The mass emissions for phase 3 (hot start) are smaller, ranging from 0.2 6 to 1.5 mg/mi. During phase 2, nearly half of the vehicles emitted ≤0.1 mg/mi, which is at the uncertainty level in the mass measurement and all emitted ≤0.7 mg/mi. These values can be compared to PM emissions from in-use vehicles recruited in the Colorado Front Range area (*30*). In that study, during the summer period, 1991−1996 model gasoline vehicles averaged 5.7, 1.8, and 2.4 mg/mi for phases 1−3 of the FTP, respectively. These are somewhat higher than the corresponding average PM emissions of 2.4, 0.2, and 0.6 mg/mi for the gasoline vehicles in the present study. This may be a result of continuing improvements in engine and aftertreatment design, which continues the trend observed in the in-use vehicle study, namely, a decrease in the three-phase FTP average emissions from 44.4 mg/mi for 1986−1990 vehicles to 2.8 mg/mi for 1991−1996 model vehicles.

Acknowledgments

We appreciate the excellent work of Mike Loos, Adolfo Mauti, and Jim Weir in setting up the dilution tunnel sampling systems and running the chassis dynamometer tests; of Dezi Lewis in determining the filter masses; of Gary Duszkiewicz in calculating and compiling the mass emissions data; and of Ema Chladek in helping with the particle size instrumentation. We thank Steve Japar, Ted Jensen, and Mark Dearth for their help and support during this investigation.

Literature Cited

(1) Dockery, D. W.; Pope, C. A. *Annu. Rev.Public Health* **1994**, *15*, 107−132.
(2) Pope, C. A.; Bates, D. V.; Raisonne, M. E. *Environ. Health Perspect.* **1995**, *103*, 472−480.
(3) Vedal, S. *J. Air Waste Manage. Assoc.* **1997**, *47*, 551.
(4) Moolgavkar, S. H.; Luebeck, E. G.; Hall, T. A.; Anderson, E. L. *Epidemiology* **1995**, *6*, 476.
(5) National Ambient Air Quality Standard for Particulate Matter: Final Rule. *Fed. Regist.* **1997**, *62*, 38652.
(6) Hildemann, L. H.; Markowski, G. R.; Jones, M. C.; Cass, G. R. *Aerosol Sci. Technol.* **1991**, *14*, 138−152.
(7) Schauer, J. J.; Rogge, W. F.; Hildemann, L. M.; Mazurek, M. A.; Cass, G. R. *Atmos. Environ.* **1996**, *30*, 3837.
(8) Cass, G. R. Report for Contract A-18-1, Coordinating Research Council, 1997.
(9) Japar, S. M. Motor Vehicles and Particle Air Pollution. *Proceedings, AWMA Symposium on Particulate Matter: Health and Regulatory Issues, Air & Waste Manage. Assoc., VIP* **1995**, *49*, 577−598.
(10) Vuk, C. T.; Jones, M. A.; Johnson, J. H. *SAE Tech. Pap. Ser.* **1976**, *No. 760131*.
(11) Dolan, D. F.; Kittelson, D. B.; Pui, D. Y. H. *SAE Tech. Pap. Ser.* **1980**, *No. 800187*.
(12) Kittelson, D. B.; Pipho, M. J.; Ambs, J. L.; Siegla, D. C. *SAE Tech. Pap. Ser.* **1986**, *No. 861569*.
(13) Baumgard, K. J.; Johnson, J. H. *SAE Tech. Pap. Ser.* **1996**, *No. 960131*.
(14) Cadle, S. H.; Mulawa, P. A.; Ball, J.; Donase, C.; Weibel, A.; Sagebiel, J. C.; Knapp, K. T.; Snow, R. *Environ. Sci. Technol.* **1997**, *31*, 3405.
(15) Greenwood, S. J.; Coxon, J. E.; Biddulph, T.; Bennett, J. *SAE Tech. Pap. Ser.* **1996**, *No. 961085*.
(16) Rickeard, D. J.; Bateman, J. R.; Kwon, Y. K.; McAughey, J. J.; Dickens, C. J. *SAE Tech. Pap. Ser.* **1996**, *No. 961980*.
(17) Maricq, M. HEI Workshop on the Formation and Characterization of Particles. *HEI Commun.* **1997**, *No 5*.
(18) Maricq, M. M.; Podsiadlik, D. H.; Chase, R. E. Presented at the 16th Annual Conference of the American Association for Aerosol Research, Denver, October 13−17, 1997.
(19) Graskow, B. R.; Kittelson, D. B.; Abdul-Khalek, I. S.; Ahmadi, M. R.; Morris, J. E. *SAE Tech. Pap. Ser.* **1998**, *No. 980528*.
(20) Dekati Ltd., Papinkatu (14−16), Fin-33200 Tampere, Finland (distributed by TSI, St. Paul, MN).
(21) Code of Federal Regulations, 40 CFR 86. Appendix I.
(22) *Off. J. Eur. Communities* **1991,** *L 242 Aug 30*, 33
(23) Gelman Sciences, 600 S. Wagner Rd, Ann Arbor, MI 48106-1448.
(24) Keskinen, J.; Pietarinen, K.; Lehtimäki, M. *J. Aerosol Sci.* **1992**, *23*, 353.
(25) Maricq, M. M.; Podsiadlik, D. H. Manuscript in preparation.
(26) Ahlvik, P.; Ntziachristos, L.; Keskinen, J.; Virtanen, A. *SAE Tech. Pap. Ser.* **1998**, *No. 980410*.
(27) Though the effect of engine temperature on gasoline engine PM emissions is not well-known, the effect on hydrocarbon emissions has been examined by Kaiser, E. W.; Siegl, W. O.; Lawson, G. P.; Connolly, F. T.; Cramer, C. F.; Dobbins, K. L.; Roth, P. W.; Smokovitz, M. *SAE Tech. Pap. Ser.* **1996**, *No. 961957*.
(28) Kittelson, D. Aerosol sampling from engines. Presented at the Symposium on particle size distribution measurement from combustion engines, Espoo, Finland, May, 1998.
(29) Maricq, M. M.; Chase, R. E.; Podsiadlik, D. H.; Vogt, R. *SAE Tech. Pap. Ser.* **1999**, *No. 1999-01-1461*.
(30) Cadle, S. H.; Mulawa, P. A.; Hunsanger, E. C.; Nelson, K.; Ragazzi, R. A.; Barrett, R.; Gallagher, G. L.; Lawson, D. R.; Knapp, K. T.; Snow, R. *$PM_{2.5}$ A Fine Particle Standard*; Proceedings from the Air & Waste Management Association Conference, Long Beach, CA, January, 1998; p 539.

Received for review August 26, 1998. Revised manuscript received February 18, 1999. Accepted February 23, 1999.

ES9808806